Mechanism of Spontaneous Inside-Out Vesiculation of Red Cell Membranes

Virgilio L. Lew, Austin Hockaday, Carol J. Freeman, and Robert M. Bookchin*

Physiological Laboratory, Cambridge University, Cambridge, United Kingdom; and *Department of Medicine, Albert Einstein College of Medicine, Bronx, NY 10461

Abstract. In certain conditions, human red cell membranes spontaneously form inside out vesicles within 20 min after hypotonic lysis. Study of the geometry of this process now reveals that, contrary to earlier views of vesiculation by endocytosis or by the mechanical shearing of cytoskeleton-depleted membrane, lysis generates a persistent membrane edge which spontaneously curls, cuts, and splices the membrane surface to form single or concentric vesicles. Analysis of the processes by which proteins may stabilize a free membrane edge led us to formulate a novel zip-type mechanism for membrane cutting-splicing and fusion even in the absence of free edges. Such protein-led membrane fusion represents an alternative to mechanisms of membrane fusion based on phospholipid interactions, and may prove relevant to processes of secretion, endocytosis, phagocytosis, and membrane recycling in many cell types.

When mammalian red cells are lysed and incubated in hypoosmotic media lacking divalent cations, their membranes spontaneously vesiculate (5, 12, 19–22, 35–37). After ~15–20 min at 37°C, freshly lysed cells yield a mixed population of inside-out vesicles (IOVs;[1] 0.05–2 μm diameter), with a variable proportion of right-side-out vesicles (ROVs) or unvesiculated "ghosts." Many of the vesicles seal to small molecules and ions, providing a convenient and much-used preparation for transport studies (5, 15, 17, 20, 22, 25, 29, 32, 39). Although the vesiculation mechanism has never been elucidated, confusing interpretations abound (40). The spontaneous vesiculation process had been followed and recorded, with highest optical resolution, using stationary specimens placed on thermally controlled slides at 37°C (21, 22). Yet the sequence of steps by which individual human ghosts transformed, in ~30 s, into a mixture of complex shapes and subsequently into free vesicles could not be explained by a coherent morphological scheme. Perhaps the most puzzling observations on record (21, 22) are those of 0.3 μm–diameter latex particles in thermal motion flowing in and out of ghosts at the same location, bouncing, while entrapped, between the inner ghost membrane and the outer aspect of any internally projecting vesicles. This ruled out simple entrapment in folds. The particles behaved as though there was a hole in the ghosts.

In the present study the transformations of red cell ghosts in sequential stages of vesiculation were followed using both thin and serial section electronmicroscopy (EM), as well as phase contrast and Nomarsky optical observations on fixed and unfixed specimens, to develop a geometrical model of the vesiculation process. It was hoped that this information would lead to working hypotheses on possible molecular mechanisms of spontaneous vesiculation.

The results showed that red cell lysis in vesiculation-inducing media generates a free membrane edge around a lytic hole which can persist for hours at low temperatures. At this stage, some membranes evert completely and form inside-out ghosts (IOGs). On incubation at 37°C, the free edges rapidly curl and lengthen to form inside-out cylinders or spiraled membrane thoroids. These break off and form IOVs by processes that involve cutting and splicing of the membrane on edge-to-side and side-to-side contacts. A molecular mechanism for this vesiculation process is proposed based on protein-led membrane fragmentation and fusion processes. The possible relevance of the present findings to mechanisms of exo- and endocytosis, phagocytosis, cell division, membrane formation and recycling, and generation of plasma membrane vesicles in vitro must now be assessed.

Materials and Methods

Fresh venous blood was obtained from normal donors using heparinized syringes. Within the range of procedural variations given below, no detectable differences were observed in the results of numerous vesiculation experiments (5, 19–22). Red cells were washed three to four times with 5–10 vol of isotonic NaCl or KCl containing 10 mM of Tris-Cl or K-Hepes buffer, pH 7.5–7.8, and 0.1 mM EGTA or EDTA to chelate extracellular divalent cations (22). The buffy coat and topmost cell layer were removed after each wash. For vesiculation the washed red cells were lysed in 40–800 vol of ice-cold solution "L" (K-Hepes, pH 7.6, 2.5 mM and EGTA, 0.1 mM). The lysed cells were immediately spun at 40,000 *g* for 15–20 min at 0–5°C. The supernatant was removed and the ghost pellet was resuspended in cold solution L (equivalent hematocrit of ~50%). For nonvesiculating controls, solution

1. *Abbreviations used in this paper*: IOG, inside-out ghost; IOV, inside-out vesicle; ROG, rightside-out ghost; ROV, rightside-out vesicle.

L with 0.1–1 mM Mg instead of EGTA was used during lysis and resuspension. Duplicate 0.1-ml samples of the ghost suspension were taken before incubation and thereafter at 30-s intervals during incubation at 37°C. To detect possible fixation or processing artifacts, a variety of procedures were used to arrest vesiculation: rapid cooling, cooling and mixing with solution L containing Mg (final concentrations 0.2–2 mM), or fixing directly with L containing 1% OsO_4. For EM studies the cold/Mg-treated samples were postfixed in 1% OsO_4 and processed as described before (18). Phase contrast and Nomarski observations were performed on fixed and unfixed samples using ×100 oil immersion objective lenses. Except for increased stiffness of fixed membranes, the optical appearance of corresponding samples treated in different ways was the same. "En bloc" uranium staining was performed following Karnovsky (16). Briefly, samples were stained at 4°C in the dark by immersion in 0.5% uranyl acetate in 0.05 M maleate buffer, pH 5.2, for 2 h. Consecutive serial sections in any figure are to be read from left to right and top to bottom, as normal text.

Results

I. Appearance of Lysed Membranes before Vesiculation

Fig. 1 shows representative optical images, EM views and serial sections of ghosts within the first 2 min of incubation at 37°C, before vesiculation occurs. Because Mg ions had been shown previously to prevent (and arrest) vesiculation (18, 20, 22, 36), red cell lysis in Mg-containing media provided controls of nonvesiculating ghosts exposed to similar conditions of tonicity, pH, temperature, ionic strength, and sample processing as vesiculating ghosts.

EM field views of cells lysed in vesiculation media (Fig. 1 *b*) show ghosts with membrane openings which are not seen in EM field views of Mg-lysed ghosts (Fig. 1 *c*). Examination of 30 Mg-lysed ghosts by serial section analysis never showed any membrane openings, in agreement with previous studies (18). On the other hand, similar analysis of 75 ghosts from cells lysed in vesiculation media showed that whenever an entire cell was contained within the sections, a membrane discontinuity, such as illustrated in Fig. 1, *h* and *i*, spanning from 2 to 30 frames (0.2–3 μm) was always observed. Similar openings were also seen in most of the partially visible ghosts. Field views or serial sections of ghosts kept for several hours in ice-cold vesiculation media were indistinguishable from those of ghosts examined within a few minutes of lysis (not shown). Phase contrast and Nomarsky views of vesiculating ghosts (Fig. 1, *a* and *j–m*) closely correspond to the EM images of open ghosts (Fig. 1, *b*, *h*, and *i*). This correspondence, together with the uniform appearance and lack of openings in Mg-lysed controls, the simultaneous presence of rightside-out and inside-out ghosts in the same samples, and the latex particle flow seen before in vesiculating ghosts (21, 22) rule out fixation or processing artifacts in the origin of the ghost openings. The surprising conclusion from these observations is that in vesiculation conditions, membrane openings and free membrane edges can persist for minutes or hours.

Mg-lysed ghosts appear either smooth or crenated (Fig. 1 *c*) whereas vesiculating ghosts, in addition to membrane openings, show large and often multiple membrane folds (Figs. 1, *a* and *b*). In EM views, all openings reveal either inward or outward edge curling (Fig. 1 *b*). To assess the sidedness of the membrane in the ghosts, use was made of the original observations of Marchesi and Palade (26) that in thin EM sections the inner membrane surface is characterized by distinctive protrusions of fibrillar material, later identified as cytoskeletal spectrin strands (28). "En bloc" uranium staining was used to compare directly inner and outer membrane surface structures. Fig. 1, *d* and *e*, show adjacent membranes from two ghosts at a region of close proximity between inner and outer membrane surfaces. Where the electrondensity of material between inner and outer membranes is similar, it can be seen that the distance between inner surfaces is about three times that between outer surfaces, consistent with the relative length of the projections extending from the top outer and bottom inner surfaces (Fig. 1 *e*). In highly magnified views of the two major types of ghosts seen in vesiculation media (Fig. 1, *f* and *g*), the inner membrane structure indicates that there are totally everted IOGs (Fig. 1 *g*) as well as rightside out ghosts (ROGs, Fig. 1 *f*). A distinctive feature of ROGs is the outward edge curling pattern whilst the more spiraled apparent inward curling pattern is indicative of IOGs. The membrane sidedness images in Fig. 1, *f* and *g*, suggest that all curling is in fact inside out.

These results document the early formation and stabilization of free membrane edges only in cells lysed in conditions which induce vesiculation. They also reveal the existence of inside-out open ghosts. Inside-out thoroidal membrane scrolls from red cells lysed in vesiculation media, with stabilized free membrane edges, were also shown by Shotton (34). These were attributed to spectrin-depleted ghosts and were not recognized as the early stage of a spontaneous vesiculation process. The dense fibrillar structure of the original inner membrane surface of ROGs and IOGs is similar to that preserved in the Mg-lysed ghosts (Fig. 1 *c*) but is largely lost in the vesicles (see Fig. 3, *d–f*). This argues against detachment of cytoskeletal components being a prerequisite for IOG formation.

II. Appearance of Membranes during the Vesiculation Process

Fig. 2 shows the three main vesiculation patterns observed during the first 2–20 min of incubation at 37°C: cup-shaped ROGs, inward-curled IOGs, and folded ROGs. Their relative proportions vary considerably in different experiments, even with cells from the same donor. The EM and optical views in Fig. 2, *a–d*, show early fragmentation images of cup-shaped ROGs and inward-curled IOGs.

Serial sections of cup-shaped ghosts and the corresponding optical images (Fig. 2, *e* and *f*) show vesicles and cylinders with apparently sealed ends extending from one pole of the cups, continuous with free membrane edges. The predominant localization of vesiculating events to a single region of the membrane is also apparent in the optical images (Fig. 2, *c–e*). Some of the large vesicles within the cups (Fig. 2, *f* and *h*) retain a pediculated link with the cup membrane (Fig. 2 *h*, insert), suggesting that these vesicles became enclosed either by endocytosis or by membrane fusion along the edge of large folds, such as those seen in folded ROGs before vesiculation (Fig. 1, *a* and *b*; see also Fig. 4 *A*). As vesiculation proceeds the cups shrink and the clusters of emerging cylinders and vesicles enlarge. The cup membranes retain the orientation and outward-curling pattern of original ROGs. This suggests that ROGs are not just transitional forms to IOGs.

Fig. 2, *a* and *b*, show inward-curled inside-out membrane fragments, indicating their origin from IOGs. Serial sections of such inward-curling fragments (Figs. 2 *g* and 3 *g*) docu-

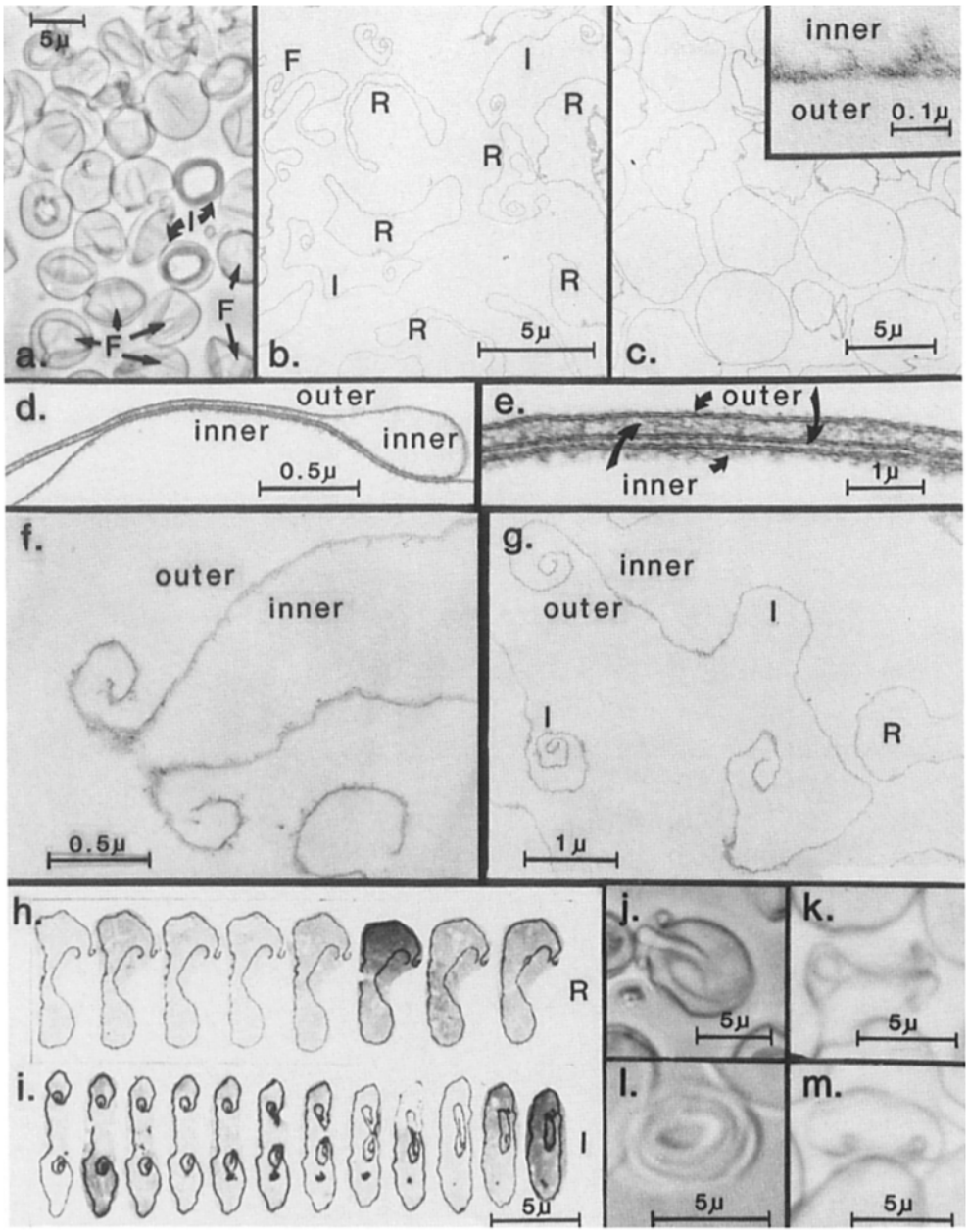

Figure 1. Appearance of red cell ghosts before or during the first 2 minutes of incubation at 37°C. *R*, Rightside-out ghost (ROG); *I*, inside-out ghost (IOG); *F*, folded ROG. *Outer* and *inner* refer to sidedness of membrane surfaces in original cell. (*a*) Phase contrast field view of ghosts after 2 min at 37°C shows multiple large membrane folds typical of early vesiculation. Note circular interiors of low optical density surrounded by optically dense thoroids in some ghosts (*I*). Comparison with the optical densities of folded and unfolded membranes of background ghosts suggests single membrane for the clear inner circles and rolled up membrane for the dense surround of the *I* ghosts, corresponding to expected frontal opening images of open ghosts with inward-curled edges as in *b*. (*b*) Thin EM field view of ghosts after 30 s at 37°C. Note the presence of membrane discontinuities with curly edges, the absence of vesicles, and the folds in the open ghosts. (*c*) Thin EM field view of Mg-lysed nonvesiculating ghosts showing no membrane openings. High magnification inset illustrates inner membrane surface projections as seen in all such ghosts. (*d*) Thin EM view of "en bloc" uranium-stained membranes (16) of two proximal ghosts. Part of the contact region is shown highly magnified in *e*. Inner membrane projections are at least three times longer than those of the outer surface. (*f* and *g*) High-magnification EM views of ghosts with outward- and inward-curling patterns of free edges. Uranium and lead staining of the sections. Inner surface fibrillar projections show that *f* is an ROG and *g* an IOG, and that all curling is inside out. (*h*, *i*, *j*, *k*, *l*, *m*) Serial EM views (*h*, *i*) and optical images (*j*–*m*) of ROGs (*h*, *j*, *k*) and IOGs (*i*, *l*, *m*), respectively.

ment continuity of the original IOG membrane with the emerging vesicles.

A third vesiculation pattern is that of ghosts filled with small vesicles (Fig. 2, *i* and *j*). High magnification (not shown) indicates that their outer membranes are rightside out, whereas the vesicles are inside out, as endocytic forms would appear. Thin and serial EM sections, however, show a fairly smooth outer membrane outline with hardly any inward budding (Fig. 2, *i* and *j*).

The serial sections of Fig. 2 *h* showed a ROG with a large internal vesicle connected to the outside by a thin residual pore. Repeated observations such as these suggest that large "endocytic" vesicles originate mainly, if not entirely, by internalization of large areas of outer membrane within fused folds, as shown in the diagram of Fig. 4 *A*. Many of the small "endocytic" vesicles, on the other hand, are open and continuous with each other or with outer membrane openings (Fig. 2, *i* and *j*). This morphology is also inconsistent with endocytic budding. Partial or total enclosure of the original membrane opening within fused folds in ROGs (Fig. 4 *A*, folded ROGs) could account for the formation of open or closed small "endocytic" forms by the same mechanisms underlying the fragmentation of outward-curling openings in cup-shaped ROGs (Fig. 2, *e* and *f*).

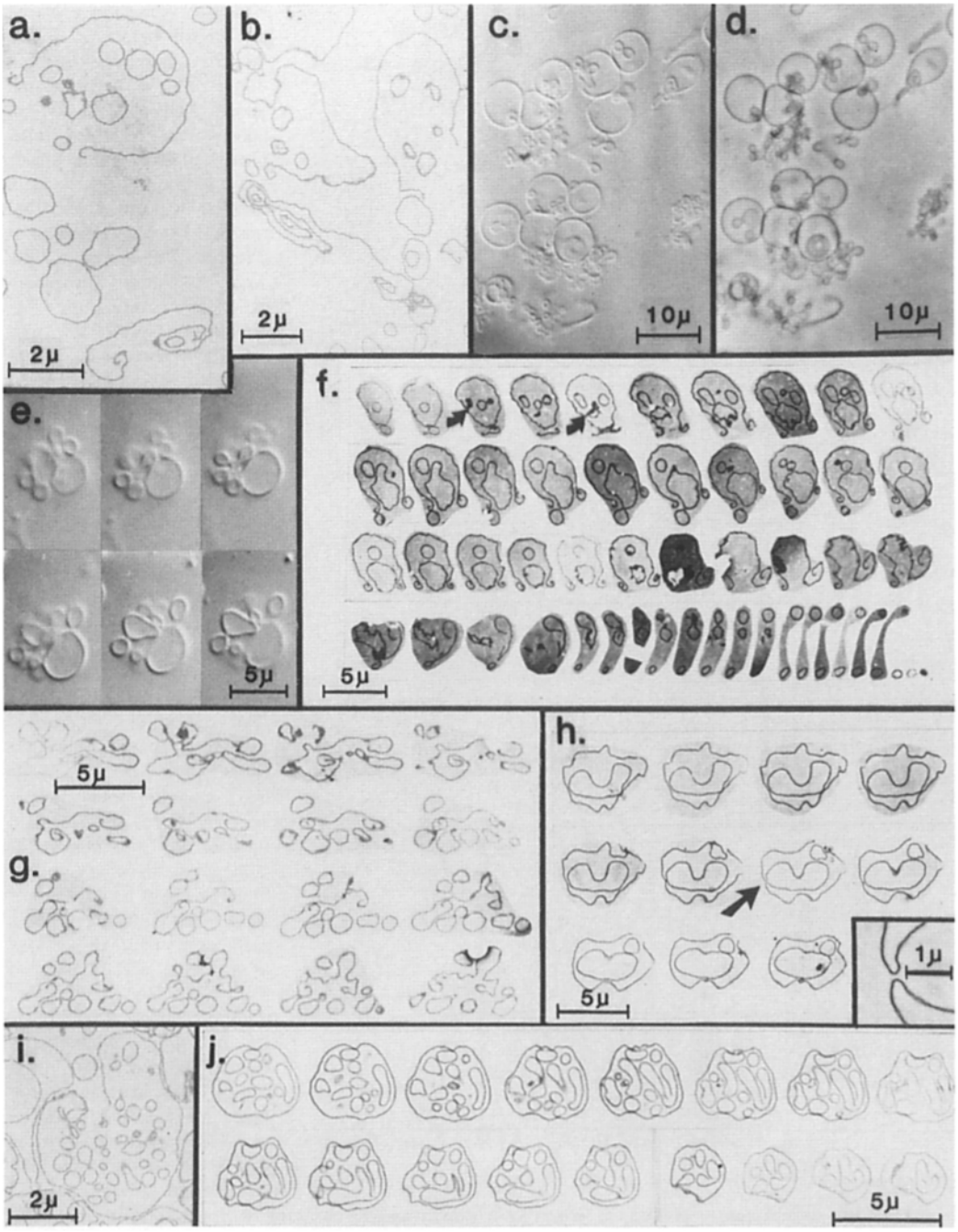

Figure 2. Appearance of fragmenting ghosts in intermediate stages of vesiculation process. Real-time video records show that vesiculation of each ghost takes ~30 s at 37°C, and there is a 2–15 min spread of initiation times (20, 22). Field views of successive intermediate vesiculation stages, therefore, document increased heterogeneity, i.e., unvesiculated ghosts, vesicles, cylinders, and fragmented ghosts are seen together (*a–d*). (*a* and *b*) EM views show conservation of cup shapes from ROGs and inward curling patterns of membrane fragments from IOGs. (*c* and *d*) Nomarsky (*c*) and phase contrast (*d*) views of a single field showing the predominant localization of vesicles towards single cell poles, and the linked appearance of most vesicles originating from a single cell. This is also shown for cup-shaped ghosts in serial Nomarsky views (*e*) and serial EM sections (*f*), and for IOGs in serial EM sections of inward-curled membrane fragments continuous with vesicles (*g*). Frequently seen membrane attachments, as within the third and fifth sections of *f* suggest that internal vesicles within the cup may originate from endocytosis or from the fusion of large folds (see also *h*). (*h*) Serial EMs of a folded ROG with large "endocytic" vesicle retaining thin connection to outer membrane (see high magnification inset of arrowed section). (*i* and *j*) Thin EM and serial EMs, respectively, of "endocytic"vesicles. Note opening of outer membrane in *i*, and fragmentations and continuities of open and closed forms in *j*.

III. Appearance of Formed Vesicles

Consecutive samples over 20 min of incubation show an increase in the proportion of vesiculating cells, and in the number of clustered or isolated cylinders and vesicles. After 20 min of incubation at 37°C, no further changes could be detected. The formed vesicles exhibit a wide variation in shape, size, and structure, the latter including open or closed, and single-, double-, or triple-layered forms (Fig. 3). The shapes

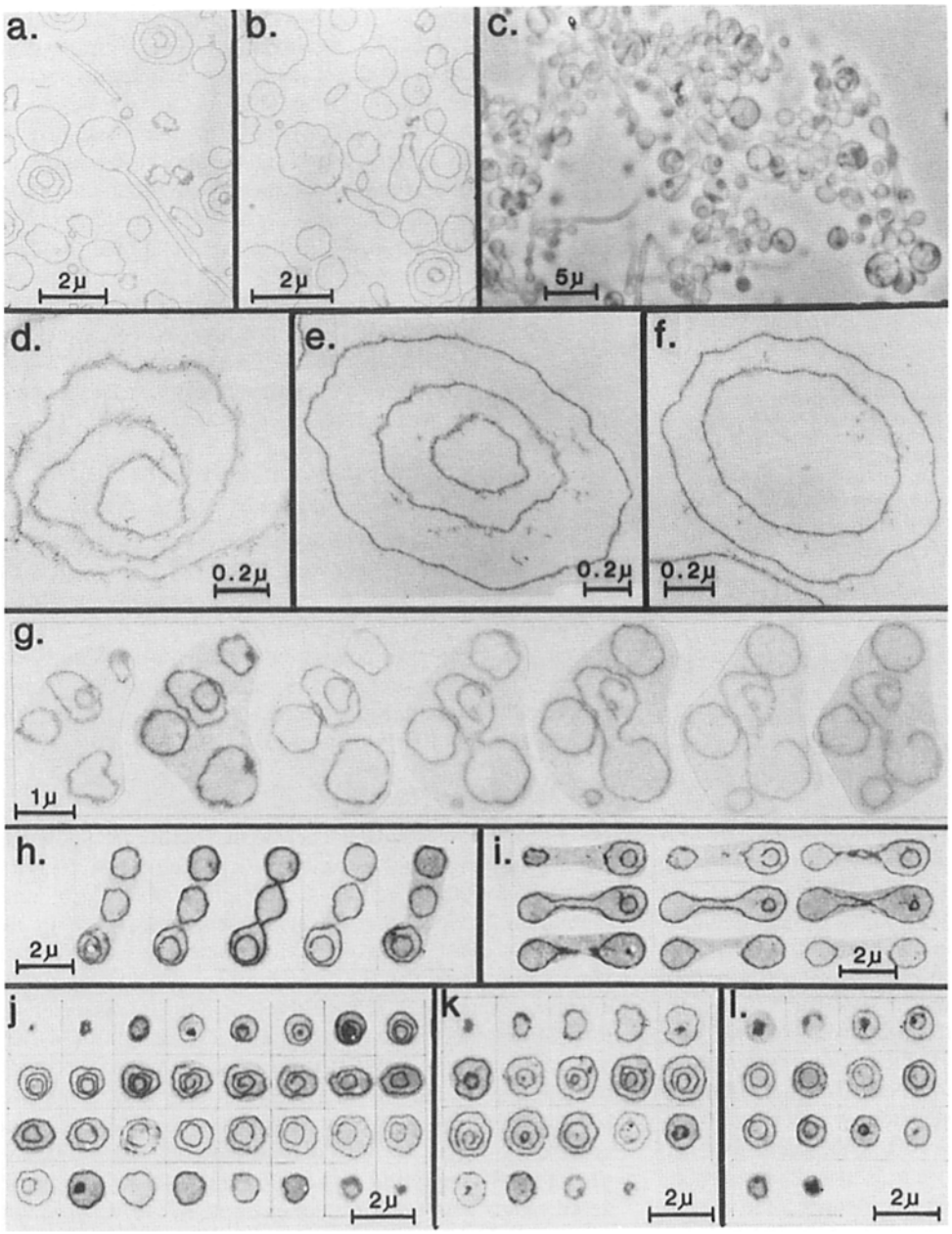

Figure 3. Appearance of vesicles formed after 20 min incubation at 37°C. (*a* and *b*) Thin EM field views show representative variety of shapes and sizes. (*c*) Phase contrast field view showing single, double and treble layered vesicles, cylindrical forms with and without constrictions, dumbbells, and vesicle-filled vesicles. (*d*, *e*, and *f*) Inward-curled spiral of IOG, treble and double vesicle, respectively, show loss of inner membrane projections in vesicles. (*g*) Double vesicle image continuous with inward-curled membrane fragment (the authors wish to stress the purely accidental nature of the presence of "Ca" in this vesicle). (*h–l*) Serial sections of open and closed vesicles.

vary from regular spheres and cylinders to combined elongated forms, with or without constrictions (Fig. 3, *a–c*) or with two or three lobes joined by small tubular bridges (Fig. 3, *h* and *i*). Some multilayered vesicles have openings in their inner or outer membranes, which often show spiral configurations (Fig. 3, *j* and *k*). The continuity between concentric vesicles and inward-curled spirals (Fig. 3, *g*, *j*, and *k*) suggests that multilayered vesicles originate from spiral membrane segments. Although much of the dense fibrillar inner membrane structure of the original ghosts (Fig. 3 *d*) had been lost by the time the vesicles were formed (Fig. 3, *e* and *f*), the inner and outer membrane surfaces could still be identified in thin sections under high magnification by careful counting of residual attached projections on each of the surfaces, avoiding areas where the plane of the section was oblique to that of the membrane. The results of such sidedness determinations on 48 vesicles (Table I) show that in most double- and triple-layered vesicles the sidedness of each membrane was inside out. Concentric vesicles, therefore, could not have originated from sequential endocytosis because this would have generated alternating inside-out and rightside-out patterns.

Discussion

I. The Geometry of Vesiculation

The typical vesiculation patterns shown in Fig. 2 indicate that budding and pinching off of endocytic vesicles can at most be only part of the vesiculation process. Because vesiculation occurs in conditions of overall conservation of membrane area, the geometrical problem may be formulated in terms of the "tailoring" required to transform the full area of

Table 1. Sidedness of Spontaneously Formed Red Cell Membrane Vesicles

Type of vesicle	Total number of each type	Membrane sidedness			Number of each form
Single	29	IO			24
		RO			3
		NC			2
		Outer	Inner		
Double	13	IO	IO		11*
		NC	NC		2
		Outer	Middle	Inner	
Treble	6	IO	IO	IO	5*
		IO	IO	NC	1

Membrane sidedness was observed in high magnification EM sections of vesicles formed after 20 min at 37°C. By this time the dense fibrillar projections which characterized initially the inner membrane surface (Fig. 1) had become more scattered (Fig. 3). Sidedness was determined by identifying residual projections attached to the inner or outer aspect of each concentric ring. IO, inside out; RO, rightside out; NC, not clear.
* Including vesicles in Fig. 3, *e* and *f*).

a cloth from ghost to vesicle through the transitional shapes observed.

A fundamental idea emerged from analyzing how concentric inside-out vesicles are generated from spiral membrane segments of fragmented IOGs, i.e., determining the maneuvers required to reconstruct, from spiral sheets, geometrical figures consistent with the consecutive transverse sections seen in Fig. 3, *j–l*. The required cutting and joining processes, shown in the diagrams of Fig. 4 *B*, row I, translate into the following membrane actions. Upon contact of the inner free membrane edge with an adjacent outer membrane surface (row I, *b* and *d*) the free edge is spliced to part of that membrane and simultaneously a new free edge is released (row I, *c* and *e*). Edge-to-edge fusion of two outer membrane borders (row I *e*) gives concentric circles in transverse section (row I *f*). Progression along the length of membrane spirals would generate concentric cylinders and vesicles with identical sidedness (Fig. 3 *l*). This mechanism can account for transformations from spirals to concentric cylinders or vesicles with conservation of sidedness, but not for the stabilization of intermediate spiral regions in some vesicles (Fig. 3, *j* and *k*). Hindrance to the progress of edge-to-side cutting-splicing may arise from surface material blocking membrane contacts. An alternative mechanism, however, is suggested by analysis of Fig. 3 *j* which shows a vesicle with a different pattern on either side of spiral sections: three concentric rings on one side and two on the other. If two separate and different contacts were formed in a membrane, the convergent approach between two conflicting patterns could generate opposing forces preventing the progress of either pattern, thus stabilizing the original spiral in the intermediate region.

The membrane motions, splicing, and cutting actions required to explain the generation of such vesicles (Fig. 3, *j–l*), can be generalized to interpret the overall vesiculation process. The diagrams of Fig. 4 *A* exemplify the vesiculation patterns seen in Figs. 1–3, whereas those of Fig. 4 *B* show the membrane events required for the observed transformations. These include side-to-side (Fig. 4 *B*, row III) as well as edge-to-side (Fig. 4 *B*, rows I and II) and edge-to-edge (Fig. 4 *B*, rows I and IV) membrane contacts. Cutting-splicing at points of contact between outer membrane surfaces within large folds would generate endocytic type vesicles in cup-shaped and folded ROGs (Figs. 2, *f* and *h*, and 4, *A* and *B*, row III). Enclosure of the original ghost opening within a fused fold would render open membrane fragments among the "endocytic" vesicles (Figs. 2 *j* and 4, *A* and *B*, row III). All side contacts observed, both with membrane folds and inside-out curling patterns, involve the outer membrane surface. Wavy or irregular direction during cutting-splicing along detaching cylinders may generate the constricted regions which give many forms a beaded appearance (Fig. 3, *a*, *c*, *h*, and *i*), and may also account for the variety of complex shapes in the emerging vesicles (Fig. 4 *A*).

II. The Molecular Mechanism: A Hypothesis

To account for the geometrical events of vesiculation it was necessary to postulate specific membrane actions underlying four distinct aspects of the vesiculation process (Fig. 4 *B*): (*a*) The forces responsible for the spontaneous membrane motions (involved in ghost eversion, edge curling, and the origin and progress of edge-to-edge, edge-to-side, and side-to-side membrane contacts); (*b*) the formation and stability of free edges; (*c*) edge elongation and reduction, and (*d*) the cutting-splicing effects of membrane contacts.

IIa. Membrane Motion

Spontaneous vesiculation occurs in conditions known to cause progressive and irreversible depletion of spectrin, the main cytoskeletal protein (2–4, 23). Irreversible loss of inner membrane projections was also documented here in the formed vesicles (Fig. 3, *d–f*). Membrane movements during vesiculation may therefore arise from potential-to-kinetic energy conversion in the regions of cytoskeletal dissociation. Rearrangements of the disintegrating cytoskeleton (24), release of membrane domains from constraining forces (9, 31), or both may determine the pattern of local movement. Despite the bewildering variety of shapes observed (Fig. 2), the recurrence of specific vesiculation patterns (Fig. 4 *A*) suggests that disintegration of the cytoskeletal frame may be ordered rather than random. An example of the way ordered disintegration may determine the cup-shape vesiculation pattern of ROGs is given in the legend of Fig. 5. The disappearance of inner-surface projections during vesiculation, however, did not follow any recognizable pattern (e.g., initial "peeling" from curled edges). Therefore, any ordered structural changes in the cytoskeleton accounting for the vesiculation patterns must precede complete detachment of spectrin–actin. In the low-ionic strength, divalent cation-free conditions required for inside-out vesiculation, short-range electrostatic interactions between surface membrane charges may also play a role in membrane movements over small distances.

IIb. A Protein Zip Mechanism

A molecular mechanism is proposed here for the stabilization, elongation-reduction, and cutting-splicing of free membrane edges, as well as for membrane fragmentation and fusion. The fundamental assumption was advanced by Shotton (34), that edge persistence implies stabilizing con-

A

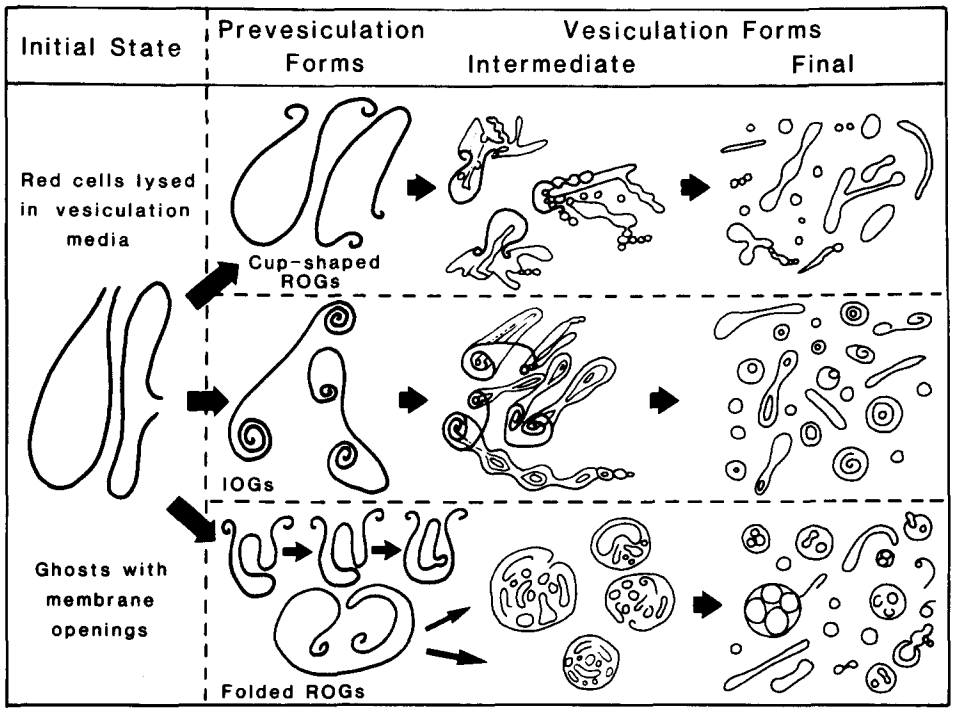

B

	Stages of Vesiculation Process	Membrane Actions	Diagrammatic Representation of Membrane Actions
I	Formation of concentric spheroids from spiral segments	Cutting-splicing on edge to side contact	a. b. c. d. e. f.
II	Detachment of closed cylinders	Cutting-splicing on edge to side contact	
	Detachment of open cylinders	Edge formation in regions of opposing forces	
III	Fragmentation of cylinders and vesicles Fusion of folds	Cutting-splicing on side-to-side contacts	Fragmentation Fusion
IV	Closing of membrane gaps	Edge reduction	

Figure 4. Diagrammatic representation of spontaneous vesiculation process. (*A*) Description of the main vesiculation patterns observed, as documented in Figs. 1-3: cup-shaped ROGs, inward-curled IOGs, and folded ROGs. (*B*) Membrane events required to interpret the geometrical transformations and fragmentations observed during the vesiculation process. Note that I-IV describe different, not sequential processes. Folds and constrictions generate side-to-side contacts only between outer membrane surfaces. Because all curls are inside out, edge-splicing is also to the outer membrane surface.

tributions from membrane proteins, and was based on the absence of stable edges in synthetic bilayers from red cell lipids. Theoretical considerations also indicate that pure lipids of any origin are extremely unlikely to form persistent free edges, even in highly artificial conditions (7, 11). The next assumption is based on available evidence suggesting that red cell membranes have abundant integral proteins which may form dimers, and whose lateral mobility is normally restricted either by direct links to the cytoskeleton or indirectly, through steric hindrances from links with other membrane proteins (6, 10, 13, 14, 30). In vesiculation conditions two basic alterations are proposed: (*a*) removal of restrictive links allowing free diffusion of the dimers in the plane of the membrane, and (*b*) a configurational change allowing the dimers to dissociate more readily. Each monomer would have a hydrophobic region buried in the fatty acid membrane core, and a hydrophilic region which can dissociate or reassociate with another monomer (see Fig. 5 *a*). In vesiculation conditions alignment of dissociated hydrophilic regions could stabilize a free membrane edge (Fig. 5 *b*). Estimates of free edge length in ROGs or IOGs before fragmentation (from serial sections, as in Fig. 1), vary widely from 2 to 20 μm. With monomers 0.2-2 nm wide, 10^4-10^5 copies would provide 20 μm of free edge. This corresponds to <10% of oligomers in band III (2, 34). The dimer-monomer transition could thus provide an effective zip mechanism, readily available anywhere on the membrane surface, able to open and splice along any lines, as determined by membrane contacts and local forces. The aligned monomers could stabilize a free edge for long periods or, after sealing a membrane by

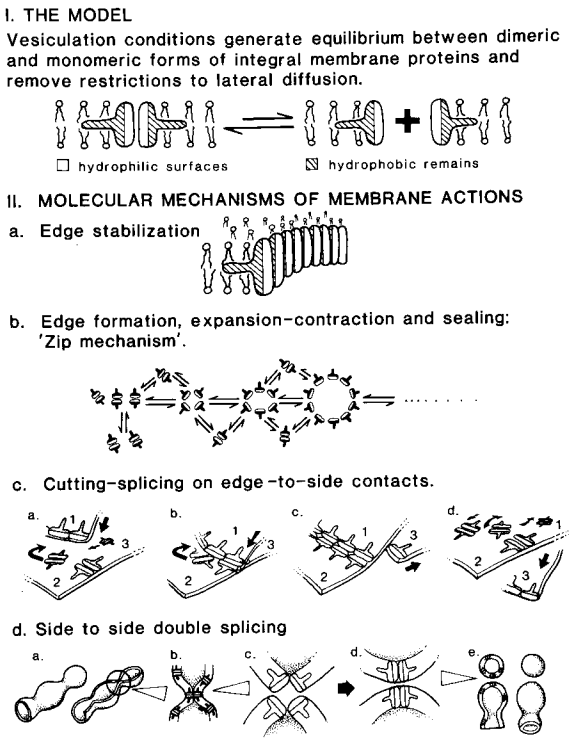

Figure 5. Molecular model of spontaneous inside-out vesiculation process. The model provides a unified explanation of the membrane events. I: Formulation of the model. Membranes are assumed to have abundant dimeric proteins with hydrophilic domains on the contact surfaces between monomers. Vesiculation conditions have two main effects on these proteins: (*a*) producing an increased rate of dissociation of dimers to monomers (which otherwise may be negligible), and (*b*) promoting cytoskeletal breakdown, thereby removing restrictions to lateral diffusion of the dimers (33). II: Molecular mechanism of membrane events during spontaneous vesiculation. Edge formation, stabilization, expansion, and reduction are represented in *a* and *b* (zip mechanism). The various cutting and splicing actions represented in *c* and *d* provide mechanisms for fragmentation and shaping of vesicles. To account for the observed vesiculation patterns (see Fig. 4 *A*), the effects responsible for spontaneous membrane motions and free dimer mobility must be coordinated in space and time. Because there is strong biochemical and morphological evidence of global spectrin-actin dissociation from the membrane during vesiculation (2–4, 23, 33 and Fig. 3), the simplest unifying assumption would be to link motions and dimer mobility to ordered functional breakdown of the cytoskeletal frame. In cup-shaped ROGs, for instance, functional cytoskeletal disintegration may occur first around the lytic hole and progress along the edge of successive fragmentations. Dimers freed locally from cytoskeletal restrictions may dissociate providing monomers for free edge elongation. Edges turn inside out following local bending forces, which generate edge-forming twists as well as the membrane contacts which result in cutting, splicing, and overall shaping of vesicles.

reassociation, disperse as laterally mobile dimers. While not unique, this molecular mechanism offers a unifying explanation of all the observed membrane behavior.

Although membrane fragments with curly free edges, as well as the formation of membrane vesicles, have been described before in plasma membrane preparations from a variety of cells (1, 8, 27, 38), including yeast, neither the temporal evolution of the free edges nor the mechanism of vesicle formation has ever been systematically investigated. Further studies will determine whether the vesiculation mechanism documented here is unique, or whether protein-led membrane interactions, such as those now proposed, participate in the generation of membrane-bound compartments in a wide range of physiological and experimental proceses. Zip-type dimer interactions on outer surface membrane contacts, for instance, could mediate the internalization of large membrane areas, as in phagocytosis or membrane recycling.

We are grateful to D. J. Lew, Vann Bennett, S. Hladky, and D. Haydon for helpful comments and discussions, to M. I. Sepúlveda and J. Gray for technical assistance, and to D. Hughes for artwork.

We wish to thank the Wellcome Trust, the Medical Research Council of Great Britain, and the National Institutes of Health (grants HL 28018 and HL 21016) for financial support and also the Department of Anatomy at Cambridge University for the use of their EM facilities.

Received for publication 21 December 1987.

References

1. Andersson, B., C. Sundby, and P. Albertsson. 1980. A mechanism for the formation of inside-out membrane vesicles. Preparation of inside-out vesicles from membrane-paired randomized chloroplast lamellae. *Biochim. Biophys. Acta.* 599:391–402.
2. Bennett, V. 1984. The human erythrocyte as a model system for understanding membrane cytoskeletal interactions. *In* Cell Membranes. Methods and Reviews. Vol. 2. E. Elson, W. Frazier, and L. Glaser, editors. Plenum Press, New York. 149–195.
3. Bennett, V., and D. Branton. 1977. Selective association of spectrin with the cytoplasmic surface of human erythrocyte plasma membranes. *J. Biol. Chem.* 252:2753–2763.
4. Bennett, V., and P. J. Stenbuck. 1979. The membrane attachment for spectrin is associated with band 3 in human erythrocyte membranes. *Nature (Lond.).* 280:468–473.
5. Bookchin, R. M., C. Raventos, and V. L. Lew. 1981. Abnormal vesiculation and calcium transport by "one-step" inside-out vesicles from sickle cell anemia red cells. Comparisons with transport by intact cells. *In* The Red Cell: Fifth Ann Arbor Conference. G. J. Brewer, editor. Alan R. Liss, New York. 163–182.
6. Cherry, R. J. 1979. Rotational and lateral diffusion of membrane proteins. *Biochim. Biophys. Acta.* 559:289–327.
7. de Gier, J., P. C. Noordam, A. J. van Echteld, J. G. Mandersloot, C. Bijleveld, A. J. Verkleij, P. R. Cullis, and B. De Kruijff. 1980. The barrier functions of membrane lipids. *In* Membrane Transport in Erythrocytes. Alfred Benzon Symposium 14. U. V. Lassen, H. H. Ussing, and J. O. Wieth, editors. Munksgaard, Copenhagen. 75–90.
8. Duran, A., B. Bowers, and E. Cabib. 1975. Chitin synthetase zymogen is attached to the yeast plasma membrane. *Proc. Natl. Acad. Sci. USA.* 72:3952–3955.
9. Evans, E. A., and R. M. Hochmuth. 1978. Mechanicochemical properties of membranes. *Curr. Top. Membr. Transp.* 10:1–64.
10. Fowler, V., and D. Branton. 1977. Lateral mobility of human erythrocyte membrane proteins. *Nature (Lond.).* 268:23–26.
11. Fromhertz, P., C. Rocker, and D. Ruppel. 1986. From discoid micelles to spherical vesicles, the concept of edge-activity. *Faraday Discuss. Chem. Soc.* 81:39–48.
12. Garcia-Sancho, J., A. Sanchez, and B. Herreros. 1982. All or nothing response of the Ca^{2+}-dependent K^+ channel in inside-out vesicles. *Nature (Lond.).* 296:744–746.
13. Golan, D E., and W. R. Veatch. 1980. Lateral mobility of band 3 in the human erythrocyte membrane studied by fluorescence photobleaching recovery: evidence for control by cytoskeletal interactions. *Proc. Natl. Acad. Sci. USA.* 77:2537–2541.
14. Golan, D. E., and W. R. Veatch. 1982. Lateral mobility of band 3 in the human erythrocyte membrane: control by ankyrin-mediated interactions. *Biophys. J.* 37:177a.
15. Grinstein, S., and A. Rothstein. 1978. Chemically-induced cation permeability in red cell membrane vesicles. The sidedness of the response and the proteins involved. *Biochim. Biophys. Acta.* 508:236–245.
16. Karnovsky, M. J. 1967. The ultrastructural basis of capillary permeability studied with peroxidase as a tracer. *J. Cell Biol.* 35:213–236.
17. Lee, K. H., and R. Blostein. 1980. Red cell sodium fluxes catalysed by the sodium pump in the absence of K^+ and ADP. *Nature (Lond.).* 285:338–339.
18. Lew, V. L., A. Hockaday, M. I. Sepulveda, A. P. Somlyo, A. V. Somlyo,

O. E. Ortiz, and R. M. Bookchin. 1985. Compartmentalization of sickle cell calcium in endocytic inside-out vesicles. *Nature (Lond.).* 315:586–589.
19. Lew, V. L., S. Muallem, and C. A. Seymour. 1980. One-step vesicles from mammalian red cells. *J. Physiol. (Lond.).* 307:36P–37P.
20. Lew, V. L., S. Muallem, and C. A. Seymour. 1982. Properties of the Ca^{2+}-activated K^+ channel in one-step inside-out vesicles from human red cell membranes. *Nature (Lond.).* 296:742–744.
21. Lew, V. L., and C. A. Seymour. 1980. Spontaneous inside-out vesiculation of lysed human red cells observed by phase-contrast microscopy. *J. Physiol. (Lond.).* 308:8P–9P.
22. Lew, V. L., and C. A. Seymour. 1982. Preparation of sealed vesicles and transport measurements. Cation transport in one-step inside-out vesicles from red cell membranes. *In* Techniques in the Life Sciences. Biochemistry, Vol. B4/1. Techniques in Lipid and Membrane Biochemistry. Part I, B415. T. R. Hesketh, H. L. Kornberg, J. C. Metcalf, D. H. Northcote, C. I. Pogson, and K. F. Tipton, editors. Elsevier/North Holland Scientific, New York. 1–13.
23. Litman, P., J. H. Chen, and V. T. Marchesi. 1978. Spectrin binds to the inner surface of the human red cell membrane via associations with band 4.1–4.2. *J. Supramol. Struct.* 8(Suppl. 2):209.
24. Lux, S. E. 1979. Spectrin-actin membrane skeleton of normal and abnormal red blood cells. *Semin. Hematol.* 16:21–51.
25. Macintyre, J. D., and J. W. Green. 1978. Stimulation of calcium transport in inside-out vesicles of human erythrocyte membranes by a soluble cytoplasmic activator. *Biochim. Biophys. Acta.* 510:373–377.
26. Marchesi, V. T., and G. E. Palade. 1967. The localization of Mg-Na-K-activated adenosine triphosphate on red cell ghost membranes. *J. Cell Biol.* 35:385–404.
27. Merkel, G. J., F. Naider, and J. M. Becker. 1980. Amino acid uptake by *Saccharomyces cerevisiae* plasma membrane vesicles. *Biochim. Biophys. Acta.* 595:109–120.
28. Nicholson, G. L., V. T. Marchesi, and S. J. Singer. 1971. The localization of spectrin on the inner surface of human red blood cell membranes by ferritin-conjugated antibodies. *J. Cell Biol.* 51:265–272.
29. Ortiz, O. E., and R. A. Sjodin. 1984. Sodium- and adenosine-triphosphate-dependent calcium movements in membrane vesicles prepared from dog erythrocytes. *J. Physiol. (Lond.).* 354:287–301.
30. Peters, R., J. Peters, K. H. Tews, and W. Bahr. 1974. A microfluorometric study of translational diffusion in erythrocyte membranes. *Biochim. Biophys. Acta.* 367:282–294.
31. Sackmann, E., H.-P. Duwe, and H. Engelhardt. 1986. Membrane binding elasticity and its role for shape fluctuations and shape transformations of cells and vesicles. *Faraday Discuss. Chem. Soc.* 81:281–290.
32. Sarkadi, B., J. Szebeni, and G. Gardos. 1980. Effects of calcium on cation transport processes in inside-out red cell membrane vesicles. *In* Membrane Transport in Erythrocytes. Relations Between Function and Structure. Alfred Benzon Symposium 14. U. V. Lassen, H. H. Ussing, and J. O. Wieth, editors. Munksgaard, Copenhagen. 220–231.
33. Schlessinger, J. 1983. Mobilities of cell membrane proteins: how are they modulated by the cytoskeleton. *Trends Neurosci.* 6:360–363.
34. Shotton, D. M. 1983. The proteins of the erythrocyte membrane. *In* Electron Microscopy of Proteins. Vol. 4. J. R. Harris, editor. Academic Press, London. 205–330.
35. Steck, T. L., and J. A. Kant. 1973. Specificity in the association of glyceraldehyde-3-phosphate dehydrogenase with isolated human erythrocyte membranes. *J. Biol. Chem.* 248:8457–8464.
36. Steck, T. L., and J. A. Kant. 1974. Preparation of impermeable ghosts and inside-out vesicles from human erythrocyte membranes. *Methods Enzymol.* 31:172–180.
37. Steck, T. L., R. S. Weinstein, J. H. Strauss, and D. F. H. Wallach. 1970. Inside-out red cell membrane vesicles: preparation and purification. *Science (Wash. DC).* 168:255–257.
38. Stroobant, P., and G. A. Scarborough. 1979. Active transport of calcium in neurospora plasma membrane vesicles. *Proc. Natl. Acad. Sci. USA.* 76:3102–3106.
39. Sze, H., and A. K. Solomon. 1979. Calcium-induced potassium pathway in sided erythrocyte membrane vesicles. *Biochim. Biophys. Acta.* 554: 180–194.
40. Wheeler, K. P. 1987. Tormented ghosts and disoriented vesicles. *Trends Biochem. Sci.* 12:177–178.